Int. J. Heat Mass Transfer. Vol. 28, No. 5, pp. 977–985, 1985
Printed in Great Britain

0017 9310/85 $3.00 + 0.00

Measurement of local mass transfer on a surface in the region of the base of a protruding cylinder with a computer-controlled data acquisition system

R. J. GOLDSTEIN, M. K. CHYU* and R. C. HAIN
Department of Mechanical Engineering, University of Minnesota, Minneapolis, Minnesota, U.S.A.

(*Received* 19 *December* 1983 *and in final form* 2 *October* 1984)

Abstract—A computer-controlled, automated data-acquisition system is employed to investigate the mass transfer characteristics of a subliming flat naphthalene surface on which a protruding cylinder is mounted with its axis perpendicular to the surface. Two cylinders with different height to diameter ratios (1 and 12) are studied. The experiments indicate that cylinder height influences the local mass transfer distribution in the region downstream of cylinder while it has little effect upstream. The average mass transfer rate over the entire measurement domain is about 8% higher with the shorter cylinder as compared to the taller one. The measurements demonstrate the automated system can provide good experimental accuracy and operating convenience.

INTRODUCTION

NAPHTHALENE sublimation in conjunction with an analogy between heat and mass transfer has been used to investigate the transfer characteristics in numerous convection-dominated heat transfer situations. Most prior studies focused on area-averaged measurements which could be conducted by weighing a naphthalene test plate before and after a run. However, in many cases, information on local transfer characteristics is of great importance, especially with regard to gaining better understanding of flow and heat transfer phenomena.

To determine the local mass transfer rates, naphthalene surface profiles are measured both before and after a mass transfer test run. Point by point subtraction of the two profiles gives the sublimed depth of naphthalene which is used in calculating the local transfer coefficient. Prior studies [1, 2, 3] indicate that the surface profile measurement procedure is tedious and time consuming. To measure approximately 300 data points might take an hour for data acquisition, and even longer for data reduction. During the data acquisition additional sublimation by natural convection can take place. In addition, human error during long and wearying measurements may lead to significant inaccuracies. To eliminate these errors, increase precision, and reduce the time required for data acquisition, an automated measurement system has been developed. The system provides vast improvement with regard to operational convenience as well as data accuracy. The main purpose of this paper is to describe the system while also showing its potency by using it to obtain significant new data for an important flow system.

Consider flow over a plate on which a circular cylinder is mounted with its axis perpendicular to the plate. The flow far from the plate corresponds to the classical two-dimensional cross flow around a cylinder, which has been subject to intensive investigation in both experiment and analysis. In terms of heat transfer the prior studies emphasized the transfer from the cylinder surface, generally presented as the average heat transfer coefficient in terms of Nusselt–Reynolds number correlations. Zukauskas [4] and Morgan [5] have compiled published results of this kind.

The present study examines the influence of a protruding cylinder on mass (heat) transfer from a flat plate. The flow in the region near the base of a cylinder has been determined by flow visualization. Mantle [6] used a smoke tracer to show the flow pattern around an isolated cylinder with height to diameter ratio of unity. Sedney [7] surveyed many previous works on the flow near small protuberances on a surface. Baker [8] measured the velocity and pressure distribution within a laminar separated boundary layer near the base of a cylinder, and reported a complex oscillatory phenomenon. Baker [9] also performed similar measurements with a turbulent flow. Langston and Boyle [10] used oil of wintergreen on a sheet to show the flow and shear stress direction on a plate surface near the base of a cylinder.

As fluid approaches the stagnation line of a cylinder in cross flow, it slows down and its pressure increases. The smaller velocity in the boundary layer on the wall on which the cylinder stands leads to a smaller pressure increase. The resulting pressure gradient parallel to the cylinder axis causes a flow toward the wall and a reverse flow upstream along the wall. The fluid rolls up forming vortices which are swept around the cylinder base, then downstream as streamwise vortex-pairs. The characteristic shape of the main vortex system has led to the name, horseshoe vortex.

Related studies of heat or mass transfer include

* Present address: Dept. of Mechanical and Aerospace Engineering, Arizona State University, Tempe, AZ 85287, U.S.A.

NOMENCLATURE

C1, C2, C3, C4 coordinates of measurement domain, see Fig. 1
d differential operator
D diameter of cylinder, 12.7 mm in present study
H height of cylinder, 12.7 mm or 152.4 mm in present study
h heat transfer coefficient, equation (1)
h_m naphthalene mass transfer coefficient, equation (2)
$\dot{m}$ mass transfer flux of naphthalene from surface
q heat flux from wall
St naphthalene mass transfer Stanton number, h_m/U_∞
St_0 naphthalene mass transfer Stanton number of flat surface without protruding cylinder
$\overline{St}$ average naphthalene mass transfer Stanton number across span $-1.8 \leqslant z/D \leqslant 1.8$
T_w temperature of wall
T_∞ temperature of freestream
t time
U_∞ velocity of freestream, 4.6 m s^{-1} in present study
X downstream distance measured from axis of cylinder, see Fig. 1
Y normal distance from X–Z plane, see Fig. 1
y distance measured from reference plane down to position on naphthalene surface
Z lateral distance across span measured from axis of cylinder, see Fig. 1.

Greek symbols

$\rho_{v,w}$ vapor mass concentration or density of naphthalene at the wall
ρ_∞ vapor mass concentration or density of naphthalene in freestream, zero in present study
ρ_s density of solid naphthalene
Δ finite difference operator.

Kruckels [11] and Jones and Russell [12] who studied local transfer distributions on annular fins. A recent study [13] of local naphthalene sublimation on a cylinder showed that the horseshoe vortex system along with the disturbed flow pattern greatly influences the mass transfer characteristics near the base of a cylinder.

HEAT AND MASS TRANSFER ANALOGY

The usual definition of heat transfer coefficient comes from the equation

$$q = h(T_w - T_\infty) \quad \text{or} \quad h = \frac{q}{T_w - T_\infty}. \tag{1}$$

Correspondingly, the mass transfer coefficient is given by

$$h_m = \frac{\dot{m}}{\rho_{v,w} - \rho_\infty}. \tag{2}$$

Analogy between equations (1) and (2) implies that $T_w - T_\infty$ and q in heat transfer are equivalent to $\rho_{v,w} - \rho_\infty$ and $\dot{m}$ in mass transfer. Eckert [14] described the principles of the analogy between heat and mass transfer processes. In the present study, the naphthalene vapor concentration in the freestream is zero and equation (2) reduces to

$$h_m = \frac{\dot{m}}{\rho_{v,w}}. \tag{3}$$

Moreover, as the mass transfer system is essentially isothermal, the naphthalene vapor pressure and vapor concentration at the surface are constant. This is equivalent to a constant wall temperature boundary condition in a heat transfer study.

Local mass transfer from a naphthalene plate can be evaluated from the change of surface elevation which is equivalent to the change in naphthalene thickness. The change of elevation or thickness due to sublimation is given by

$$dy = \frac{\dot{m}\, dt}{\rho_s} \tag{4}$$

where ρ_s is the density of solid naphthalene. Note that dy and $\dot{m}$ are functions of local coordinates of the plate, i.e. both X and Z. Combining equations (3) and (4), and integrating over the test duration yields

$$h_m = \frac{\rho_s \Delta y}{\rho_{v,w} \Delta t}. \tag{5}$$

The mass transfer Stanton number is defined by

$$St = \frac{h_m}{U_\infty}. \tag{6}$$

If, as is often the case, the wall temperature varies slightly during test run, ρ_{vw} can be represented by the time-averaged naphthalene concentration at the surface. This is obtained from numerical integration of the concentrations determined at the measured surface temperature. A correlation, in a form of third degree Chebyshev polynomial interpolation, proposed by

Ambrose *et al.* [15] is used to determine naphthalene vapor pressure, from this, $\rho_{v,w}$ is evaluated using the ideal gas law and the wall temperature.

EXPERIMENTAL APPARATUS AND PROCEDURE

Wind tunnel and test plate

The experiments are carried out in a specially designed open-circuit wind tunnel installed in the University of Minnesota Heat Transfer Laboratory. The tunnel has an entrance section which includes screens and flow straighteners followed by a contraction section, a test section, a diffuser, a blower and discharge duct.

The test section of the tunnel has a uniform cross-section 203 mm high by 152 mm wide, and is 838 mm long. A turbulent boundary layer is induced on the test wall by placing at the end of the contraction section of the tunnel a 2 mm diameter wire trip followed by a 45 mm strip of 120 grade sandpaper. The test plate with the naphthalene covering 120 × 190 mm is shown in Fig. 1. The leading edge of the naphthalene mass transfer active region is 330 mm downstream of the trip wire. The freestream velocity U_∞ and boundary-layer velocity profiles are determined using a total pressure probe and static pressure wall taps. With U_∞ maintained at 4.6 m s^{-1} for all runs, boundary-layer velocity profiles are measured in the absence of a cylinder and with an aluminum flat plate substituted for the naphthalene surface. The boundary layer at a location 42 mm upstream from where the cylinder axis is to be placed can be characterized as equivalent to a fully turbulent boundary layer. The measured boundary-layer thickness (where velocity is 0.99 U_∞) and displacement thickness are 8 mm and 1.2 mm respectively at this location. The Reynolds number based on the cylinder diameter and U_∞ is about 4000.

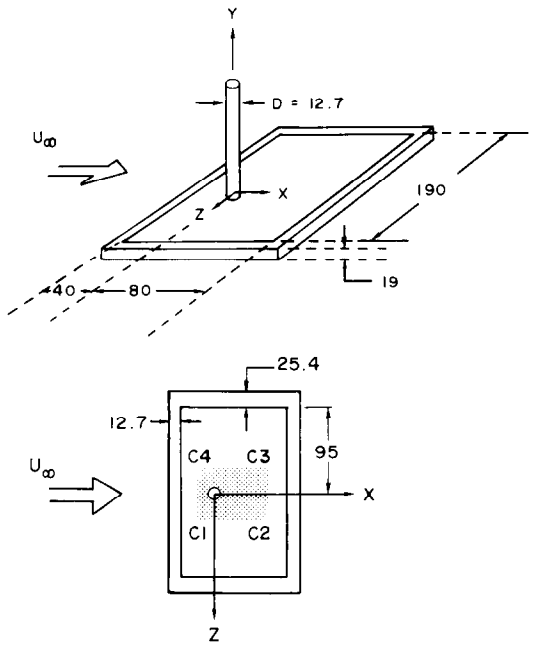

FIG. 1. Test plate. Units in mm; shaded area represents measurement domain:

	X/D	Z/D
C1	−1.5	1.8
C2	4.5	1.8
C3	4.5	−1.8
C4	−1.5	−1.8

The cast naphthalene region is obtained by placing the test plate in an inverted position on a highly polished aluminum flat plate and then pouring the hot (near boiling point) naphthalene liquid into molding holes. After the system cools down to near room temperature, a sharp blow on the side of the polished plate separates it from the naphthalene coated surface.

In order to have the cylinder standing firmly on the naphthalene plate during the test run, a teflon annulus with O.D. equal to that of the cylinder is inserted into the cylinder base hole. One end of the cylinder is machined to fit the I.D. (6.3 mm) of the annulus ensuring a firm support.

Two brass cylinders with identical diameter, D = 12.7 mm, but with different heights, are used, their heights are 1 and 12 diameters respectively. The test plate along with the mounted cylinder are exposed to the wind tunnel air flow for about 150 min.

The naphthalene vapor concentration on the surface is the driving force of the mass transfer process. To determine the naphthalene vapor concentration and pressure, temperatures are measured every 5 min during a test run. A teflon insulated, 0.25 mm (0.01 in) diameter, cooper–constantan thermocouple is used to measure the naphthalene surface temperature. The thermocouple is inserted into the test plate from the back side of the plate prior to the naphthalene casting process. After casting, the thermocouple is held firmly by the solidified naphthalene and its junction is nearly flush with the subliming surface. During a test run, the measured naphthalene surface temperature is found to be lower than the freestream temperature by 0.2°C or less.

Automated data acquisition system

Precise positioning, accurate surface elevation reading, and rapid data acquisition are decisive factors to ensure successful local measurement in sublimation studies. A computer-controlled measurement apparatus was designed and installed to fulfill these requirements. A block diagram giving a schematic view of the entire arrangement is shown in Fig. 2.

The system consists of a depth gauge along with a signal conditioner, a multimeter, two stepper-motor driven positioners, a hardware unit for motor control, an HP-85 microcomputer, and a PDP-11/34 minicomputer system.

For precise positioning, a system with two single-axis, lead-screw driven, perpendicularly located positioners is installed. This system can locate the depth gauge on the naphthalene plane (X–Z) by controlling

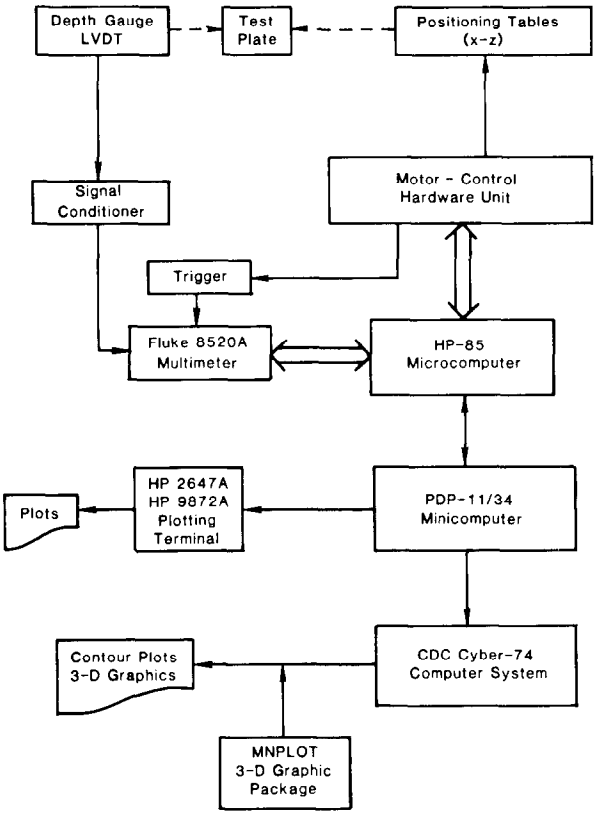

FIG. 2. Automated data acquisition system.

combined movements of each positioner. Both positioners have the same travel range, 457 mm (18 in.). However, for practical purposes, the carrying surface areas are different. The smaller one (152 × 70 mm) manufactured by Velmex Inc. carried the depth gauge while the larger one (635 × 380 mm), made by Design Components Inc., which could provide more stable mechanical movements carried the test plate. A sketch of the positioning system is shown in Fig. 3.

The digitally controlled motors are from Superior Electric Company, model number SLO-SYN MO-63. They are capable of rotating their shafts 200 steps rev^{-1} with a noncumulative 3% error per step increment. In conjunction with the pitch of the lead-screw, each step increment of the motor causes the positioner to move 0.0254 mm (0.001 in.). An HP-85 microcomputer along with a program coded in BASIC language and its I/O interface commands serves as a controller to the movements of the stepper-motors. The bounds of the rectangular measurement region in terms of X and Z and the values of ΔX and ΔZ between each measurement can be put into the HP-85 computer program. This computer then controls the number of steps of the stepper motors to change location on the plate by these ΔX and ΔZ increments during the measurements.

For a complete motor-control process, it is essential to place an interfacing component between the controller and the motor which is capable of converting the controller's commands in digital form into a number of properly sequenced phase control signals needed to physically move the stepper-motors. The hardware unit serving as this interface is the Superior Electric Company produced MODULYNX motion control system. It contains five electronic circuit cards including one interface card connected in series with the two-axis system using an indexer card and a driver card for each axis. Those cards are mounted in a common chassis along with the necessary power supplies and switches.

The depth gauge used to measure the naphthalene surface profile is a Schaevitz Engineering produced linear variable differential transformer (LVDT) which is calibrated against precision gauge blocks to obtain 0.5 mm linear range and about 2.54×10^{-5} mm (1.0×10^{-6} in.) resolution. This resolution is 2–3 orders of magnitude smaller than the operating range of measured naphthalene sublimation. The LVDT is connected to an electronically compatible signal conditioner (CAS-025) which supplies excitation and converts the A.C. signal output of the gauge to a D.C. voltage, and allows necessary adjustment and calibration by the user. The output of the conditioner is calibrated to provide a signal of 1 V per 0.0254 mm (0.001 in.).

For data acquisition, one may consider that a

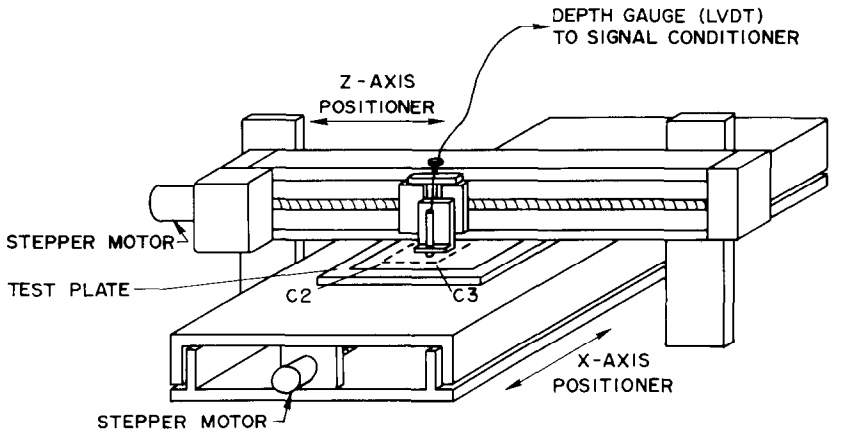

FIG. 3. Positioning system.

measurement cycle starts when the motors have received the programmed command from the controller, and then moved the depth gauge to a designated location on the naphthalene surface. This location is represented by X and Z coordinates. After an adjustable delay period of 0.1–1 s, a trigger signal from a custom-made trigger circuit is generated. On receipt of the trigger signal, the multimeter reads the voltage output of the conditioner and displays it digitally. The motion-complete trigger signal simplifies programming, ensures the system having synchronized operation throughout the whole measurement process, and optimizes the rate of data acquisition. The value of y determined by the multimeter is transferred to the HP-85 through the IEEE-488 bus. The X and Z coordinates had been predetermined in the program. Moreover, the data are transferred out of the HP-85 via a RS-232 interface connection to a PDP-11/34 minicomputer for further data reduction and evaluation. This concludes a single measurement cycle, and the system is now ready to instruct the motors to begin the next movement. This repeatable measurement process ends when all the designated locations on the naphthalene surface have been visited.

The measurement procedure for the present experiment is programmed to go over a rectangular area on the X–Z plane with specified step lengths in both directions. It covers an area of 45.7 mm (Z-axis) by 76.2 mm (X-axis) on the naphthalene surface with a total of 1025 (25×41) discrete points and takes approximately 18 min for data acquisition and storage.

Data reduction procedure

Measurements of the naphthalene surfaces profiles are taken before and after exposure in the wind tunnel. The change in naphthalene thickness or depth sublimed is determined by taking the difference of the two measured surface elevations at given (X, Z) position.

To obtain the surface profile, a datum plane is determined by recording all the spatial coordinates (X, y, Z) at any three reference points on the metal part of the test plate. Then the naphthalene surface elevation at any designated point can be evaluated as the measured y-coordinate in reference to that of the same point on the datum plane. The controller, HP-85 microcomputer, stores the (X, Z) coordinates of each reference point for the purpose of ensuring the same three points will be visited after a test run. The same reference plane presumably is obtained so long as the identical set of reference points are used on the non-subliming surface. A number of preliminary tests showed this assumption is valid to an extent of less than 2% error of the average sublimation depth. The average sublimation depth is about 0.05 mm (0.002 in.).

Most of the data reduction procedures are conducted with the PDP-11/34 minicomputer. A graphics subsystem including a Hewlett Packard 2647A graphics terminal and 9872A plotter are directly connected to the PDP-11/34, so results from the measurements can be plotted if desired. Nevertheless, for the present study, the reduced data were also transferred from the PDP-11/34 to the University Computer Center CDC Cyber-74 main frame computer. The Cyber system equipped with a three-dimensional graphic package, MNPLOT allows the user to generate three-dimensional plots.

RESULTS AND DISCUSSION

The mass transfer distributions are normalized using measurements made on a flat naphthalene plate without a protruding cylinder in the same tunnel operating with the same flow parameters. On this plate the local Stanton number, St averaged over the span (Z) of the plate (there is actually little variation along Z), shows a power law dependency on the streamwise coordinate (X), $St_0 \sim X^{-0.18}$. This compares favorably with a correlation recommended by Reynolds *et al.* [16] for heat transfer from a flat plate to a turbulent

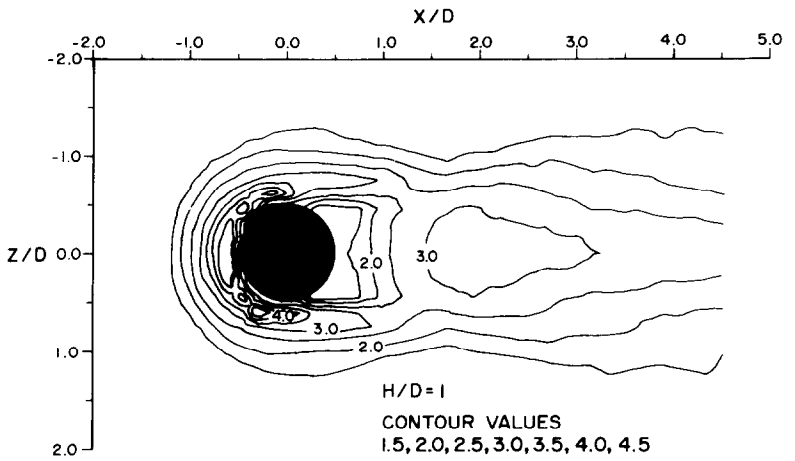

FIG. 4. St/St_0 for short cylinder, $H/D = 1$.

boundary layer with zero freestream pressure gradient, though the absolute values of Stanton number are somewhat less probably due to the inactive starting length. The influence of the protruding cylinder on the wall mass transfer is presented in terms of a point-by-point ratio of the Stanton number with or without the cylinder present, St/St_0. Contour plots of St/St_0 for the two geometries ($H/D = 1$ and 12) are shown in Figs. 4 and 5. Figure 6 shows three-dimensional projection plots of St/St_0 viewed from downstream of the cylinder toward the upstream direction. Figure 7 presents the spanwise-averaged (for $-1.8 \leqslant Z/D \leqslant 1.8$) mass transfer coefficient in the form of $\overline{St}/St_0$. This includes the area with zero mass transfer under the cylinder. Figures 8 and 9 show the variation of St/St_0 along the streamwise direction (X/D) at several Z locations.

The mass transfer upstream of the cylinder is little affected by the difference in cylinder height. With either cylinder St/St_0 is close to unity until about one diameter upstream of the cylinder's leading edge. Downstream of this location St/St_0 increases with X along the line of symmetry ($Z/D = 0$) reaching a maximum about $0.2D$ ahead of the cylinder surface. In addition to the upstream maximum at $Z/D = 0$, there are two symmetrically located local maxima, one on each side of the cylinder. The mass transfer variation can be qualitatively explained by reference to the flow pattern. The boundary layer of the approaching flow separates in a three-dimensional manner, and induces a secondary flow wrapped around the base of the cylinder creating a horseshoe vortex system. This flow produces high shear stress on the wall beneath it, accordingly, St/St_0 is large. Within the three-dimensional separated boundary layer, the pressure field causes fluid to skew around the cylinder in a helical fashion creating vortices with a streamwise component.

Immediately downstream of the cylinder, relatively little mass transfer occurs, this is a recirculation region with low speed air flow. At larger X, St/St_0 increases with distance downstream along the line of symmetry

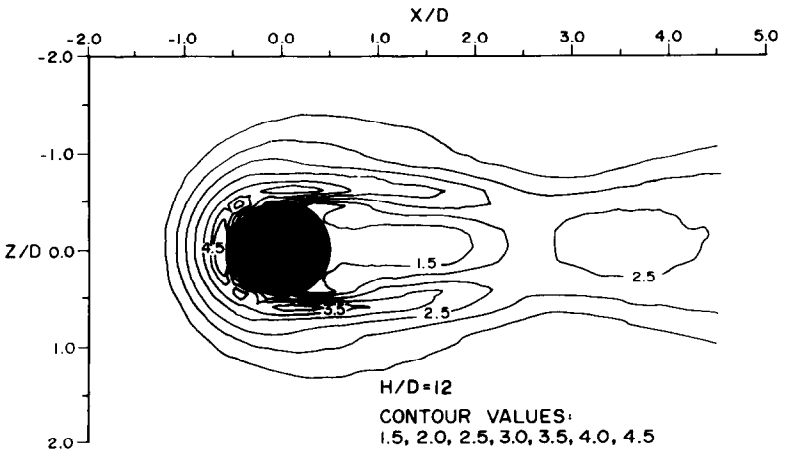

FIG. 5. St/St_0 for tall cylinder, $H/D = 12$.

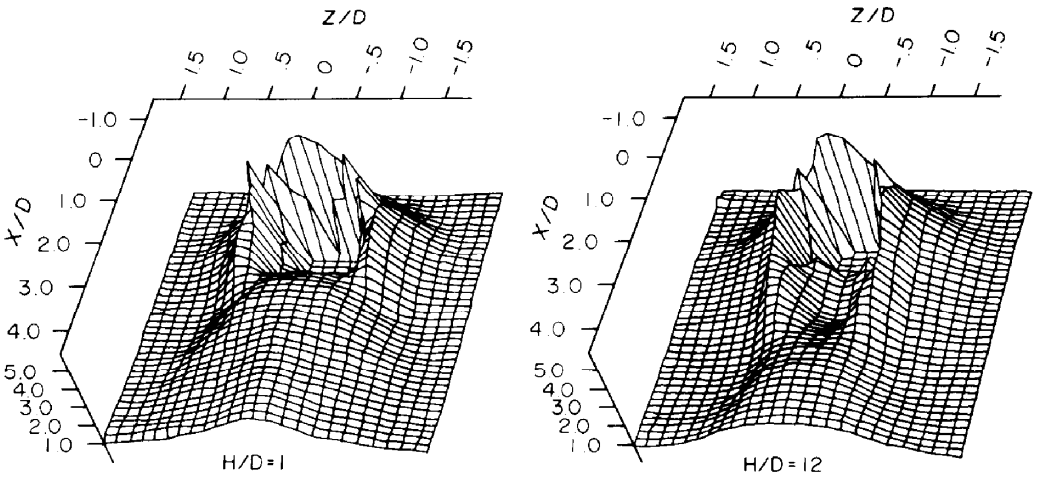

FIG. 6. Three-dimensional projected view of St/St_0.

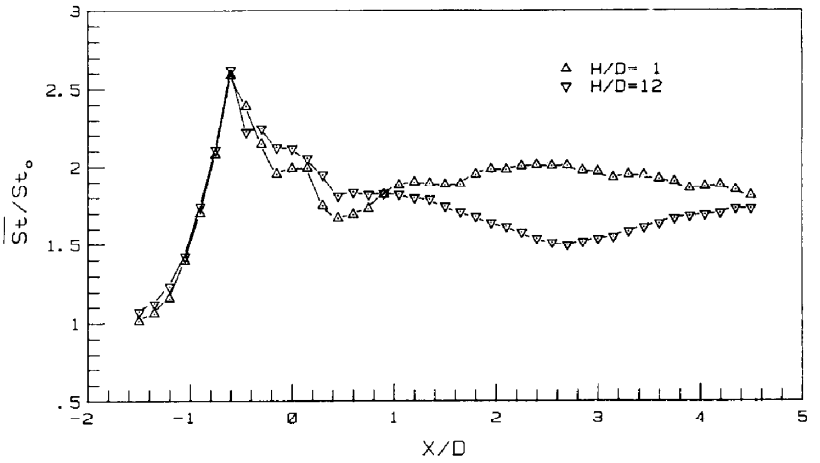

FIG. 7. Stanton number averaged across span, $-1.8 \leqslant Z/D \leqslant 1.8$.

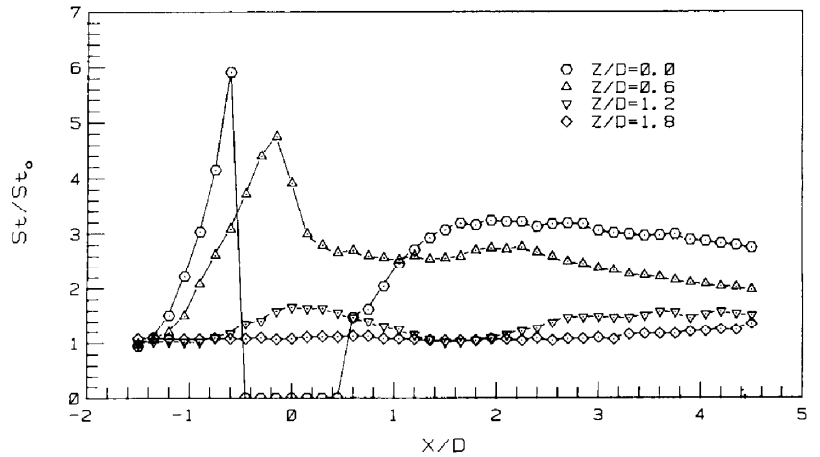

FIG. 8. Local Stanton number for short cylinder, $H/D = 1$.

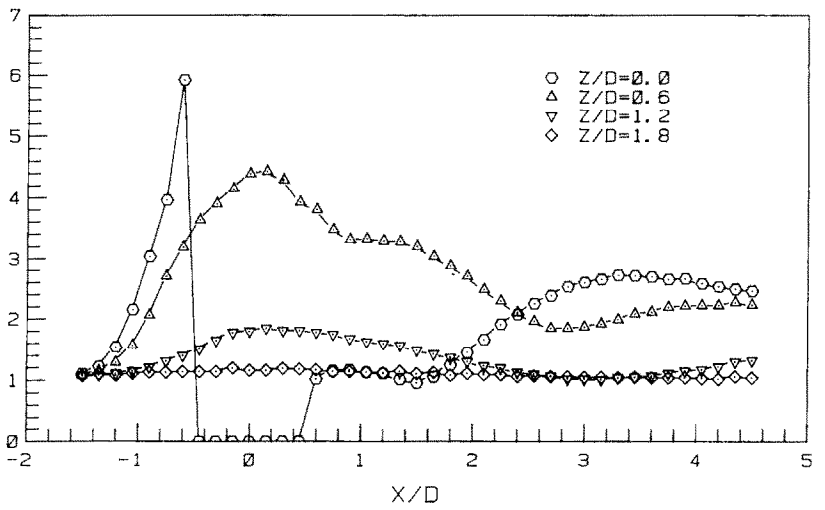

FIG. 9. Local Stanton number for tall cylinder, $H/D = 12$.

reaching another maximum in the reattachment zone. Although the recirculation region and local maxima are present with both geometries, their characteristics, sizes and shapes are quite different for the two different cylinders. For $H/D = 1$, the flow separates from the top edge of the cylinder and creates a shear layer with high entrainment into the recirculation region. The curvature of these streamlines results in strong turbulent eddies and shear stress, this reduces the length of the recirculation region and enhances the mass transfer in the reattachment zone. Reattachment, as determined from the rise in mass transfer coefficient, is at about $1.5D$ and $3.0D$ downstream of the downstream edge of the short and tall cylinders respectively. Values of St/St_0 in the reattachment zone are about 15–20% greater with the shorter cylinder than with the taller one.

The very high mass transfer rate adjacent to the cylinder persists further downstream in the case of the taller cylinder. However, at most Z locations the effects of increased mass transfer extend further downstream with the shorter cylinder. Thus the spanwise-averaged mass transfer ($-1.8 \leqslant Z/D \leqslant 1.8$) is larger with the shorter cylinder for X/D greater than about 1.0. The influence of a small, but very intense vortex indicated by the mass transfer from a cylinder near its base [13] was not observed on the wall in the present study. This may be due to different flow conditions; for instance, much smaller Reynolds number in present work, or larger sizes of probe tip and step increment in the present study as compared to ref. [13].

The value of the mass transfer averaged over the entire measurement domain ($-1.5 \leqslant X/D \leqslant 4.5$; $-1.8 \leqslant Z/D \leqslant 1.8$) was determined by numerical integration. This area averaged mass transfer rate divided by that on the surface with no cylinder present is 1.85 for the short cylinder and 1.68 for the tall one (note that this includes the area under the cylinder where the mass transfer is zero when the cylinder is present).

CONCLUSIONS

A computer-controlled automated data-acquisition system is very effective for rapid and precise measurement of local convective (subliming) mass transfer in the region of a cylinder–wall interaction. Extension of the system to non-flat geometries is also possible.

The present experimental results show the effects of a horseshoe vortex flow around a circular cylinder protruding from a flat surface exposed to a uniform freestream. Quantitative information on the effect of surface mass transfer is obtained. Different cylinder heights (1 and 12 diameters) provide different mass transfer distributions. A non-uniform mass transfer rate along with a number of local maxima are observed immediately in front of the cylinder, along the side of the cylinder and downstream of the cylinder. In the downstream region, higher mass transfer generally occurs with the shorter cylinder as compared to the taller one.

Acknowledgement—Support from the U.S. Department of Energy Engineering Research Program was instrumental in the conduct of the work reported herein.

REFERENCES

1. H. H. Sogin and V. S. Subramanian, Local mass transfer circular cylinders in cross flow, *J. Heat Transfer* **83**, 483–493 (1961).
2. F. E. M. Saboya and E. M. Sparrow, Local and average

transfer coefficients for one-row plate fin and tube heat exchanger configurations, *J. Heat Transfer* **96,** 265–272 (1974).
3. R. J. Goldstein and J. Taylor, Mass transfer in the neighborhood of jets entering a crossflow, *J. Heat Transfer* **104,** 715–721 (1982).
4. A. Zukauskas, Heat transfer from tubes in crossflow, *Advances in Heat Transfer*, Vol. 8. Academic Press, New York (1972).
5. V. T. Morgan, The overall convective heat transfer from smooth circular cylinder, *Advances in Heat Transfer*, Vol. 11. Academic Press, New York (1975).
6. P. L. Mantle, A new type of roughness heat transfer surface selected by flow visualization techniques, *Proc. 3rd Int. Heat Transfer Conference*, Vol. I, pp. 45–55 (1966).
7. R. Sedney, A survey of effects of small protuberances on boundary-layer flows, *AIAA J.* **11,** 782–792 (1975).
8. C. J. Baker, The laminar horseshoe vortex, *J. Fluid Mech.* **95,** 347–367 (1979).
9. C. J. Baker, The turbulent horseshoe vortex, *J. Wind Engng Ind. Aero.* **6,** 9–23 (1980).
10. L. S. Langston and M. T. Boyle, A new surface-streamline flow-visualization technique, *J. Fluid Mech.* **125,** 53–58 (1982).
11. W. W. Kruckels, Determination of local heat transfer coefficients in forced convection air flow by aid of photometric measurements, *AIChE Symposium Series*, No. 68, pp. 112–118 (1972).
12. T. V. Jones and C. M. B. Russel, Heat transfer in annular fins, ASME Paper 78-HT-30 (1978).
13. R. J. Goldstein and J. Karni, The effect of a wall boundary on local mass transfer for a cylinder in cross-flow, *J. Heat Transfer* **106,** 260–267 (1984).
14. E. R. G. Eckert, Analogies to heat transfer processes, in *Measurements in Heat Transfer* (edited by E. R. G. Eckert and R. J. Goldstein). Hemisphere Publishing, New York (1976).
15. D. Ambrose, I. J. Lawenson and C. H. S. Sprake, The vapor pressure of naphthalene, *J. chem. Thermodynam.* **7,** 1173–1176 (1975).
16. W. C. Reynolds, W. M. Kays, and S. J. Kline, Heat Transfer in the turbulent incompressible boundary layer I—constant wall temperature, NASA Memo. 12-1-58W (1958).

MESURE DU TRANSFERT MASSIQUE LOCAL SUR UNE SURFACE AU VOISINAGE DE LA BASE D'UNE EXCROISSANCE CYLINDRIQUE AVEC UN SYSTEME D'ACQUISITION DE DONNEES

Résumé—Un système automatique d'acquisition de données est utilisé pour étudier les caractéristiques du transfert de masse sur une surface plane de naphtalène en sublimation sur laquelle une excroissance cylindrique est posée avec l'axe perpendiculaire à la surface. Deux cylindres, avec des rapports hauteur sur diamètre différents, sont étudiés. Les expériences indiquent que la hauteur du cylindre influence la distribution du transfert massique dans la région inférieure du cylindre tandis qu'elle a un effet très faible au sommet. Le flux massique moyen sur le domaine complet de mesure est environ 8% plus élevé avec le cylindre plus court, par rapport au plus long. Les mesures montrent que le système automatique peut fournier une expérimentation commode et précise.

AUTOMATISCHE MESSUNG DES ÖRTLICHEN STOFFÜBERGANGS AN EINER OBERFLÄCHE, AUS DER EIN ZYLINDER SENKRECHT HERAUSRAGT

Zusammenfassung—Ein computergesteuertes automatisches Meßwerterfassungssystem wird eingesetzt, um den Stoffübergang einer sublimierenden flachen Naphthalinschicht zu untersuchen, auf welcher ein senkrecht hervorstehender Zylinder befestigt ist. Zwei Zylinder mit verschiedenen Verhältnissen von Höhe zu Durchmesser (1 und 12) werden untersucht. Die Experimente zeigen, daß die Zylinderhöhe die örtliche Stoffübergangsverteilung im stromabwärts gelegenen Gebiet des Zylinders beeinflußt, während sie stromaufwärts wenig Einfluß zeigt. Der mittlere Stoffübergangskoeffizient über das gesamte Meßgebiet ist ungefähr 8% größer beim kürzeren Zylinder, verglichen mit dem längeren Zylinder. Die Messungen zeigen, daß man mit dem automatischen Meßwerterfassungssystem eine gute experimentelle Genauigkeit und einen bequemen Meßablauf erreichen kann.

ИЗМЕРЕНИЯ ЛОКАЛЬНОГО ТЕПЛООБМЕНА НА ПОВЕРХНОСТИ У СОСНОВАНИЯ ВЫСТУПАЮЩЕГО ЦИЛИНДРА С ПОМОЩЬЮ АВТОМАТИЗИРОВАННОЙ СИСТЕМЫ

Аннотация—Для исследования характеристик массопереноса сублимирующей поверхности нафталина, на которой установлен выступающий цилиндр, ось которого перпендикулярна поверхности, применяется автоматизированная система контроля и обработки информации. Исследованы два цилиндра с различными отношениями высоты к диаметру (1 и 12). Опыты показали, что высота цилиндра влияет на распределение локального массообмена вниз по течению, тогда как вверх по течению это влияние незначительно. Средняя скорость массопереноса во всей области измерений на 8% выше у низких цилиндров по сравнению с высокими. Измерения показывают, что автоматизированная система обеспечивает хорошую точность эксперимента и удобна в работе.